Field Emission of Spin-Polarized Electrons Extracted from Photoexcited GaAs Tip

2006 Jpn. J. Appl. Phys. 45 6245

(http://iopscience.iop.org/1347-4065/45/8R/6245)

Japanese Journal of Applied Physics
Vol. 45, No. 8A, 2006, pp. 6245–6249

Field Emission of Spin-Polarized Electrons Extracted from Photoexcited GaAs Tip

Makoto KUWAHARA*, Tsutomu NAKANISHI, Shoji OKUMI, Masahiro YAMAMOTO, Masaharu MIYAMOTO, Naoto YAMAMOTO, Ken-ichi YASUI, Takanori MORINO, Ryousuke SAKAI, Kuniaki TAMAGAKI and Koichi YAMAGUCHI[1]

Graduate School of Science, Nagoya University, Nagoya 464-8602, Japan
[1]*Department of Electronic Engineering, University of Electro-Communications, Chofu, Tokyo 182-8585, Japan*

(Received February 18, 2006; revised April 13, 2006; accepted May 1, 2006; published online August 4, 2006)

A pyramidal-shaped GaAs (tip-GaAs) photocathode for a polarized electron source (PES) was developed to improve beam brightness and negative electron affinity (NEA) lifetime by field emission. The emission mechanism also enables the photocathode to extract electrons from the positive electron affinity (PEA) surface into vacuum, and alleviates the NEA lifetime problem. The measured electrical characteristics of tip-GaAs and its polarization exhibited distinctive field-emission behavior. The polarization of the electron beam extracted from tip-GaAs was 20–38% under irradiation with circularly polarized light of 700–860 nm, and the peak polarization was $37.4 \pm 1.4\%$ at a wavelength of 731 nm. These experimental results indicate that spin-polarized electrons can be extracted from the conduction band into vacuum by a field-emission mechanism. This, in turn, shows that this type of photocathode has the prospect of generating a low-emittance spin-polarized electron beam. [DOI: 10.1143/JJAP.45.6245]

KEYWORDS: spin-polarized electron, field emission, photocathode, circularly polarized laser, GaAs, anisotropic etching, photolithography, depolarization

1. Introduction

Spin-polarized electron sources are necessary for applications in high-energy physics and material science.[1–5] Advances in PES photocathodes have led to the development of a GaAs–GaAsP strained superlattice photocathode that is capable of generating high polarization, high quantum efficiency, and a multi bunch time-structure beam.[6–9] However, two major problems remain, namely, the improvement of beam emittance and the settlement of the NEA surface lifetime problem. This photocathode requires advanced techniques of ultrahigh vacuum and the reduction in dark current because of the NEA surface.[10] Consequently, a new method for avoiding NEA surface lifetime is needed. To overcome both problems simultaneously, we started to develop a tip-GaAs photocathode that would enable the use of the field-emission mechanism. Using the tip-GaAs photocathode, electrons can be emitted from a small area at the tip of the pyramid, which is expected to minimize beam emittance.

The generation of polarized electrons is explained by the following three-step model. First, circularly polarized light illuminates onto a GaAs-type semiconductor for selective electron excitation. Secondly, conduction band electrons are diffused to the surface area. Finally, excited electrons are extracted from the surface into vacuum. In the third step in this study, we employed the field-emission mechanism as a substitute for the NEA surface. We measured the current–voltage (I–V) characteristics and the experimental spin polarization (ESP) spectrum of the tip-GaAs photocathode by field emission with an optical orientation. Furthermore, we analyzed the mechanism of field emission of this photocathode by examining the dependence of spin polarization on excitation photon energy.

2. Experimental Procedure

2.1 Photocathode preparation

A pyramidal-shaped GaAs was fabricated from a p-type GaAs(100) substrate (Zn-doped $2 \times 10^{19}\,\mathrm{cm}^{-3}$) by anisotropic wet etching using H_3PO_4 solutions.[11] For GaAs etching, resist-mask patterns were prepared on the GaAs substrates by photolithography. The feature of the resist pattern was a square, 10 µm on a side. The edge of the square mask was aligned along the ⟨010⟩ direction. To sharpen the tip radius, GaAs etching was carried out in a $10H_3PO_4 + H_2O_2 + H_2O$ solution at $-1\,^{\circ}\mathrm{C}$. As shown in Fig. 1, the sample had a tip radius of about 25 nm, and a tip-to-tip distance of 200 µm. After etching, the sample was rinsed by HCl–isopropanol treatment to remove gallium and arsenic oxides from the surface.[12]

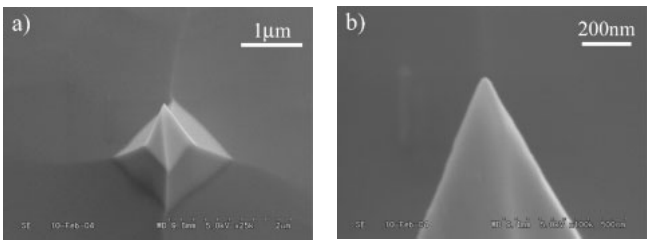

Fig. 1. SEM images of tip-GaAs fabricated by anisotropic wet etching: (a) overview of pyramidal-shaped GaAs (tip-GaAs) and (b) magnified image of pointed tip.

2.2 Instruments

In this experiment, we used a 20-kV DC gun for detailed measurements of field-emission current, and a 70-keV PES for spin polarization measurement. The reason for using the 20-kV DC gun is that the 70-kV DC gun cannot apply sufficient high-electric field to measure field-emission characteristics from tip-GaAs. Conversely, ESP measurement was taken by a 70-keV PES, because the 20-kV DC gun did not have a spin polarization analyzer. This equipment was maintained under a ultra high vacuum (10^{-9} Pa) conditions to create a NEA surface. Each chamber was evacuated by an ion pump and a nonevaporable getter (NEG) pump. The 20-kV gun is schematized in Fig. 2. The

*E-mail address: kuwahara@spin.phys.nagoya-u.ac.jp

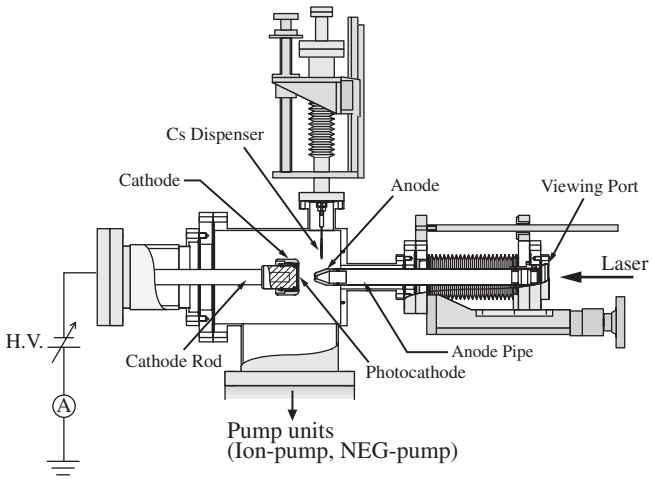

Fig. 2. Schematic of 20-kV DC gun.

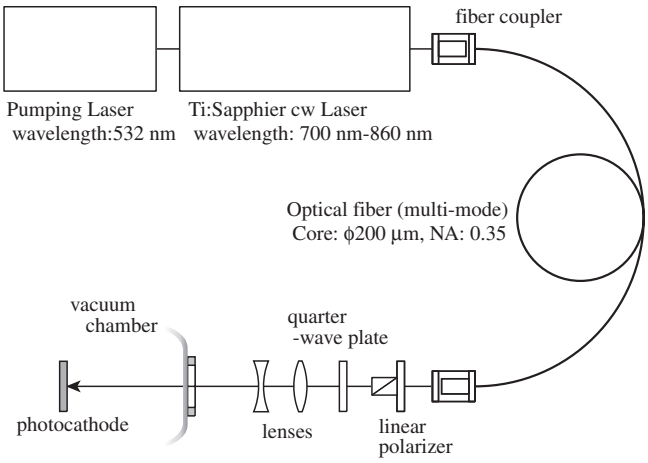

Fig. 3. Optical setup for applying circularly polarized light.

electrodes were made of stainless steel 316L because they have a relatively low carbon content that can cause a site of field emission of dark current. For surface polishing, electrochemical etching and buffering were employed simultaneously to obtain a mirror-flat surface.[10,13] The photocathode sample was attached to a molybdenum stage, and heated using a rod heater to remove the arsenic layer and obtain a clean surface. Cesium was evaporated from a commercially available dispenser that was placed in front of the cathode by a manipulator during the cesiation process. Oxygen was introduced into the gun chamber from a pure oxygen tank through a variable leak valve. The gap separation between the cathode and the anode was variable because the anode was supported by a manipulator equipped with a viewing port. Circularly polarized light was directed into the photocathode surface through the viewing port. This apparatus could supply a high-gradient dc electric field of 4.8 MV/m to the photocathode surface because the gap separation of the electrodes and the applied voltage were 3.2 mm and 20 kV, respectively, under conditions where the dark current did not exceed 0.1 nA despite the amount of cesium deposited on the cathode during the many cesiation processes. The electric field is smaller than the value obtained by dividing the voltage by the gap, because the geometry of the electrodes is not a flat plate. The actual electric field was estimated by using the electromagnetic simulation code POISSON with the electrodes' geometries and dimensions.

The 70-keV PES was composed of a 70-kV DC gun and a spin polarization analyzer. The spin polarization measurement system contains a Wien-filter and a Mott scattering polarization analyzer (Mott-polarimeter). The DC gun of PES is designed to use a photocathode that is illuminated with a laser light. The electron beam generated from the DC gun is transferred to the Mott-polarimeter through the Wien-filter. This apparatus is described in more detail in ref. 7.

The optical arrangement for the measurement of spin polarization and quantum efficiency (QE) is shown in Fig. 3. Light from the Ti:sapphire cw laser (Spectra Physics 3900) was guided to a circular polarizer, which consists of a linear polarizer and a quarter-wave plate, by a multimode optical fiber with a core diameter of 200 μm and a numerical aperture of 0.35. After the circular polarizer, the circularly polarized light illuminates a sample mounted on a cathode of the DC gun. The laser spot diameters at the photocathode of the 20-kV DC gun and 70-keV PES are 3 and 14 mm, respectively.

3. Results

I–V characteristics were measured using a 20-kV DC gun under illuminating circularly polarized light. At first, we measured the field emission of photoexcited tip-GaAs samples without surface activation. However, the emission current could not be observed under the application of a high-electric field of 4.8 MV/m with illumination by He–Ne laser light (wavelength = 633 nm, power = 4 mW). Thus, in the present experiment, to obtain a small PEA surface, cesium was employed to reduce the surface potential barrier. After the deposition of cesium, we continued to monitor QE until it stopped decreasing and the surface condition was stabilized, under a low applied voltage of 200 V and He–Ne laser irradiation. After that, we used the small PEA surface condition. Figure 4 shows the Fowler–Nordheim (F–N) plots of the emission current obtained by laser light irradiation at a

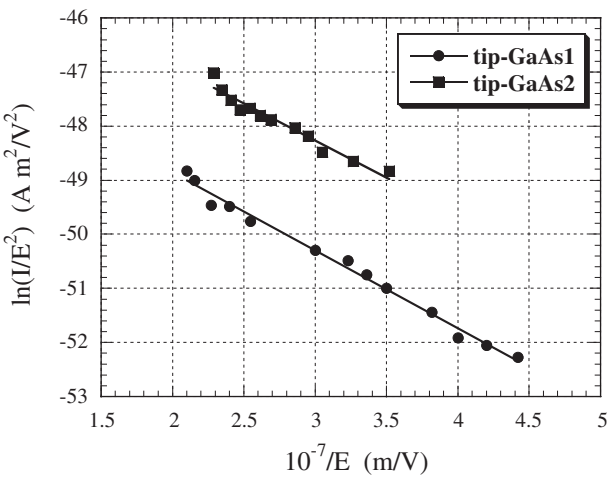

Fig. 4. *I–V* characteristics of photocurrent extracted from tip-GaAs. Emission current data plotted in F–N coordinates. The solid lines represent the least-squares fit to the F–N equation.

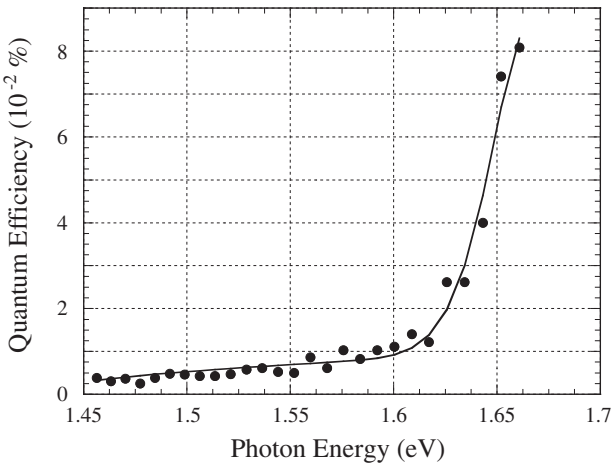

Fig. 5. QE of tip-GaAs under high applied gradient field (2.9 MV/m) as function of excitation photon energy. The solid line shows the fit to the tunneling yield calculated from the WKB approximation.

wavelength of 780 nm. The F–N plot is a two-dimensional plot of $\ln(I/E^2)$ vs $1/E$, where I is an emission current and E is an electric field, and is often used for predicting a field-emission phenomenon. The solid lines in Fig. 4 show the least-squares fits of the experimental data. The two plots showed a difference in the QE results. These plots had a similar slope, but the extracted current density was different. Thus, the two fitting lines had the same slope because the coefficient of the enhancement factor of these shapes was the same. The slopes of the fitting lines were $(1.4 \pm 0.6) \times 10^7$ and $(1.4 \pm 0.2) \times 10^7$ in SI units.

The QE spectrum of tip-GaAs under high dc gradient was measured. Figure 5 shows QE as a function of excitation photon energy under a high gradient field of 2.9 MV/m; the applied voltage and electrode gap were 20 kV and 5.34 mm, respectively. The solid line is the fitting curve obtained through a calculation of tunneling yield based on the WKB approximation. The QE increased rapidly at 1.6 eV, which did not correspond to the band-gap energy of GaAs. The QE of NEA-GaAs increased more gradually, which was reflected in the joint density of state.

ESP measurements of tip-GaAs were made using a Mott-polarimeter with a 70-kV DC gun. Figure 6 shows the ESP and QE of tip-GaAs under a high applied gradient field and concurrent irradiation with a circularly polarized laser light. For clarifying these ESP measurement conditions, each QE that was taken together with the ESP measurement by the 70-keV PES is plotted with the horizontal axis. The ESP curve for tip-GaAs shows a bumpy profile between 20 and 38% with an excitation photon energy of 1.44 to 1.77 eV. Furthermore, the ESP spectrum has higher values than that of NEA-GaAs in the photon energy range above 1.61 eV. This energy range corresponds to the rising edge of QE at 1.6 eV. This photon energy also coincided with the value in Fig. 5.

4. Discussion

We analyzed the results using the extraction process model shown in Fig. 7. The combination of the axis in the F–N plot is derived from the Fowler–Nordheim equation,[14] which can be expressed as

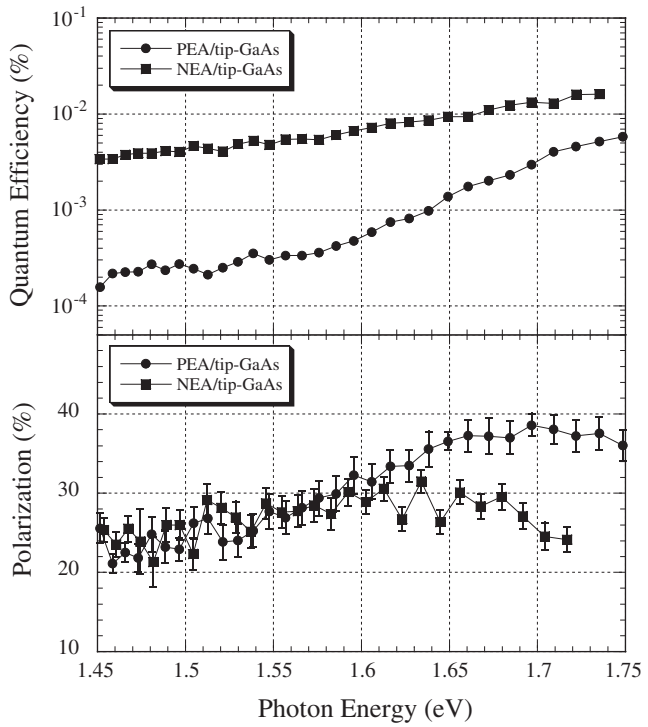

Fig. 6. ESP and QE of tip-GaAs (PEA and NEA) as functions of excitation photon energy.

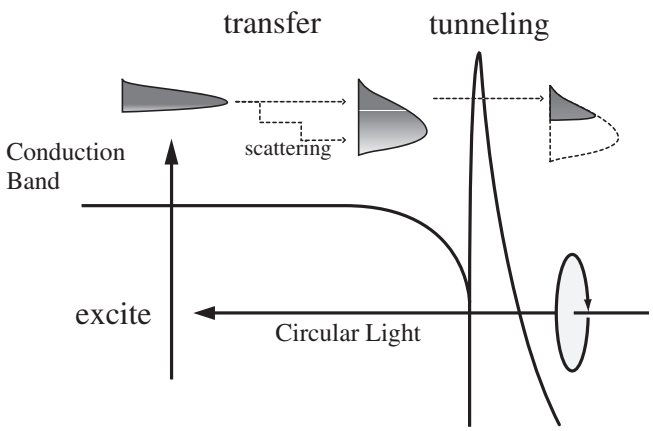

Fig. 7. Schematic of one-dimensional potential model of field emission in p-doped semiconductor. The magnitude of polarization is indicated by the light and shaded regions under the energy distribution curve, where darker shades correspond to higher polarization.

$$J = 1.54 \times 10^{-6} \frac{(\beta E)^2}{\chi} \exp\left(-6.87 \times 10^7 \frac{\chi^{3/2}}{\beta E}\right), \quad (1)$$

where J is the current density, E is the electric field, β is a field enhancement factor, and χ is the electron affinity. In Fig. 4, the data could be well fitted by the straight line. Hence, the proportional behavior to the F–N plot suggests that excited electrons were extracted into vacuum by the tunneling effect. Furthermore, an electron affinity can be also calculated from the slope of the fitting curve in the F–N plot using eq. (1). From this equation, the electron affinity is estimated to be $(1.6 \pm 0.5) \times 10^{-2} \cdot \beta^{2/3}$ using the slope of the fitting curve in Fig. 4, which was taken to be $(1.4 \pm 0.5) \times 10^7$ in the present calculation. The magnitude of β

depends on the geometry and demensions of the cathode. For a tip curvature of 50 nm and a tip-to-tip distance of 200 μm, the field enhancement factor β of tip-GaAs is estimated to be 66 by using the simulation code POISSON. In this estimation, electric field infiltration into the semiconductor is not considered because of the high p-doping density. Hence, the electron affinity of tip-GaAs was estimated to be 0.26 ± 0.08 eV.

The fitting curve by the WKB approximation in the QE spectrum in Fig. 5 can be expressed as

$$T(\varepsilon_z) = \exp\left[-\frac{4\sqrt{2m}}{3\hbar eE}(\chi - \varepsilon_z)^{3/2}\right]. \quad (2)$$

Here, T is the tunneling yield, ε_z is the electron energy, m is the electron mass, and e is the elementary electron charge. Considering the correspondence of the fitting curve in Fig. 5, the rapid increase reflects a surface tunneling effect. Thus, the phenomena demonstrated that excited electrons were extracted by the field-emission mechanism. Subsequently, from the result of the QE spectrum, electron affinity was also estimated by the WKB approximation fitting. Taking the band-gap energy of GaAs at 300 K to be 1.43 eV, the electron affinity is estimated to be 0.23 ± 0.01 eV from the fitting curve parameter.[15] This estimate is in good agreement with the estimate obtained by the F–N plot. Thus, the two estimations based on the tunneling effect are consistent with each other, which indicates clearly that the spin-polarized electrons were extracted by field emission. Furthermore, the relation between the I–V characteristics and the QE spectrum was established.

In Fig. 6, the ESP data at the PEA surface condition had a difference from the NEA surface condition in the photon energy range above 1.6 eV. The QE spectrum at the PEA surface condition increased rapidly at 1.6 eV. This behavior corresponds to the aforementioned discussion of QE spectrum. Thus, the ESP data at the PEA surface condition above 1.6 eV was identified as a field-emission condition with that of QE spectrum. Consequently, Fig. 6 shows that the behavior of ESP at the field-emission condition differed from that at the NEA condition. This experimental result indicates that the spin-polarized electrons can be extracted from the conduction band into vacuum through the GaAs tip without serious depolarization. To understand this phenomenon, firstly, we considered the depolarization mechanism in a GaAs crystal. The Bir–Aharonov–Picus (BAP) process and the D'Yakonov–Perel (DP) process have been identified as the main mechanisms of spin relaxation of photoexcited electrons in p-type GaAs.[16] While drifting to the surface, partial excited electrons are scattered by holes and phonons among others.[17,18] Electrons that were photoexcited to the bottom of the conduction band could be transported to the surface with little scattering. Furthermore, scattering by holes occurred mainly during depolarization, which was caused by the BAP process. On the other hand, when electrons are excited above the bottom of the conduction band, they are scattered while drifting to the surface. Such hot electrons are scattered with mainly phonons, and largely through the DP process.[19] It seems that the energy dispersion widens, and the low-energy end of this wide dispersion has a lower polarization compared with the initial polarization. Because the tunneling yield of a surface increases at a rapid rate for electron energy, electrons transmitting into vacuum constitute the majority of the high-energy end of the wide dispersion. Consequently, it would appear that the low-polarization portion is cut off, and the high-polarization portion can only extract into vacuum. Thus, a high polarization could be obtained. Furthermore, the extracted electron beam, which is expected to have a narrow energy dispersion, suggests that the initial beam emittance is reduced.[20,21]

To confirm that the effective QE is higher than the observed QE, we calculated diffusion length. The diffusion length of conduction band electrons can be estimated using a diffusion coefficient and lifetime (recombination relaxation time). Diffusion length is expressed as $\sqrt{D\tau}$, where D is the diffusion coefficient of conduction band electrons, and τ is the lifetime of conduction band electrons. The lifetime τ is 96 ps, as reported in ref. 22, and the diffusion coefficient is estimated to be 2.6×10^{-3} m^2/s using the minority-electron mobility of 1000 cm^2 V^{-1} s^{-1} in 1×10^{19} cm^{-3} doped p-GaAs.[23–25] Thus, the diffusion length is estimated to be 4.9×10^2 nm. The depth from which excited electrons could arrive to the surface is equal to the diffusion length. This means that the electrons extracted from tip-GaAs come from within a 500 nm radius of the tip. Thus, the irradiating laser light was only effective when used in the vicinity of the pyramid tip. The effective QE was estimated from the extraction depth of excited electrons. It is estimated that the effective excitation area has a diameter of 1 μm. The effective QE was estimated to be about 7×10^2-fold larger than that of the whole illuminated area using as parameters a tip radius of 50 nm and a tip-to-tip distance of 200 μm. For example, using the data shown in Fig. 6, the effective QE was estimated to be about 1% at 1.7 eV. This shows that the effective QE of tip-GaAs is in agreement with that of NEA-GaAs.

These results have demonstrated the usability of the spin-polarized electron source; however, problems were encountered, namely, the small field-enhancement factor and the melting problem of tip-GaAs. When the current exceeded 1 μA with an illuminating laser light whose diameter was about 3 mm, several tops of the tips melted and broke off since we examined the melting phenomena caused by high current density at the top of a tip. The high current density produced an increase in temperature of tip-GaAs by joule heating. We calculated the temperature using an equation of heat conduction and the feature of tip-GaAs samples. In a thermal equilibrium situation, the following equation can be used.

$$\lambda \nabla^2 T + H = 0 \quad (3)$$

Where T is a temperature, H is a heat current and λ is a coefficient of thermal conductivity. Considering the effect of heat transfers, eq. (4) can be expressed as

$$\frac{d}{dx}\left(\lambda S(x)\frac{dT(x)}{dx}\right) = \frac{\rho I^2}{S(x)} - 2\pi\sigma T^4\sqrt{S(x)}. \quad (4)$$

$S(x)$ is a cross-sectional area as a function of x, which is a distance measured from the emission point of a tip. I is a current, ρ is an electrical resistivity and σ is the Stefan–Boltzmann constant. To estimate the joule heating effect with heat transfers of conduction and radiation, we assumed

a tip curvature radius of 50 nm, an aspect ratio of 5, and a substrate temperature of 300 K. The other coefficients used, which are related to GaAs properties, are shown in ref. 15. The temperature of the pointed tip was estimated to exceed 1250 °C, which is the melting point of GaAs at a current of about 47 nA from a tip. At a current of 26 nA, the temperature is roughly estimated to be 400 °C, which can be stable without arsenic evaporation.

In the present experiment, a PEA surface was used because the electrical field enhancement effect was not sufficient. Generally, the field enhancement factor β is required to be 300 for field emission because the field emission of GaAs needs to be about 1 GV/m given that the electron affinity of GaAs is about 4 eV. However, the PEA surface, which takes sufficient time after the deposition of cesium, is stable compared with the NEA surface. Thus, a generation of spin-polarized electrons using field emission has a practical value as a method of relaxation for the NEA surface lifetime problem. Indeed, once a small PEA surface was obtained, QE decreased from 9×10^{-5} to 2×10^{-5} for 41 d, in which the apparatus used was a 70-keV PES, a laser light wavelength of 725 nm and an applied voltage of 70 kV.

The brightness of the electron beam extracted from a single tip was not measured in this study, but this value can be roughly estimated. We assume the following parameters; an electron affinity χ of 0.23 eV, a field gradient of 4 MV/m, a top curvature radius of 50 nm, and an emission current I of 10 nA. Finally, the voltage ΔV, which is equivalent to the initial energy, is 0.1 eV. Using these conditions and the F–N equation, the emission area is estimated to be about 5 nm in diameter. Thus, the beam angle α_c and the beam radius at the virtual crossover point r_c are about 0.01 rad and 5.9 nm, respectively. In this calculation, we used the sphere-on-cone model for an approximate calculation based on a computer simulation.[26] The brightness B can be written as $B = I/\pi\alpha_c^2 \cdot \pi r_c^2$. Thus, the brightness of the electron beam is calculated to be $2.8 \times 10^7\,\mathrm{A\,cm^{-2}\,sr^{-1}}$. This brightness estimate suggests that tip-GaAs operates similarly to normal field emission type electron sources. Tip-GaAs cannot generate a high current, but it can produce a high-brightness beam. Furthermore, in contrast to the present photocathode, a normal photocathode cannot extract such a narrow beam because of the diffraction limit of the excitation light. Thus, the present tip-GaAs cathode is highly effective as a PES.

5. Conclusions

We have demonstrated that spin-polarized electrons can be extracted from tip-GaAs using a field-emission mechanism under circularly polarized light irradiation. The polarization of the electron beam extracted from tip-GaAs was between 20 and 38%. Furthermore, singular phenomena caused by field emission were observed in the QE and ESP spectra. The polarization was higher than that of NEA-GaAs above 1.6 eV. In addition, the QE curve rose rapidly. Moreover, the effective QE of tip-GaAs approached that of NEA-GaAs. In conclusion, we regard tip-GaAs with field emission as a spin-polarized electron photocathode that can produce a low emittance and achieve long lifetime because it avoids the use of a NEA surface. It is hoped that this photocathode will be widely applicable to high-energy accelerators and analytical instruments such as an electron microscope.

Acknowledgements

The authors extend their gratitude to T. Gotoh and M. Katsuki of Nagoya University for their valuable support. This work was supported in part by a Grant-in-Aid for Scientific Research (No. 15204019) from the Ministry of Education, Culture, Sports, Science and Technology of Japan and a research fund of KEK for cooperative development of polarized electron sources (1998–2002) and low-emittance electron sources (2003–2004).

1) C. Y. Prescott, W. B. Atwood, R. L. A. Cottrell, H. DeStaebler, Edward L. Garwin, A. Gonidec, R. H. Miller, L. S. Rochester, T. Sato, D. J. Sherden, C. K. Sinclair, S. Stein, R. E. Taylor, J. E. Clendenin, V. W. Hughes, N. Sasao, K. P. Schüler, M. G. Borghini, K. Lübelsmeyer and W. Jentschke: Phys. Lett. B **77** (1978) 347.
2) M. Meyerhoff *et al.*: Phys. Lett. B **327** (1994) 201.
3) SLD Collaboration: Phys. Rev. Lett. **74** (1995) 2880.
4) R. Zdyb and E. Bauer: Phys. Rev. Lett. **88** (2002) 166403.
5) T. Kohashi and K. Koike: Jpn. J. Appl. Phys. **40** (2001) 1264.
6) T. Nishitani *et al.*: J. Appl. Phys. **97** (2005) 094907.
7) K. Togawa *et al.*: Nucl. Instrum. Methods Phys. Res., Sect. A **414** (1998) 431.
8) K. Togawa *et al.*: Nucl. Instrum. Methods Phys. Res., Sect. A **455** (2000) 118.
9) S. Tanaka, T. Nishitani, T. Nakanishi, S. D. More, J. Azuma, K. Takahashi, O. Watanabe and M. Kamada: J. Appl. Phys. **95** (2004) 551.
10) F. Furuta, T. Nakanishi, S. Okumi, T. Gotou, M. Yamamoto, M. Miyamoto, M. Kuwahara, N. Yamamoto, K. Naniwa, K. Yasui, H. Matsumoto, M. Yoshioka and K. Togawa: Nucl. Instrum. Methods Phys. Res., Sect. A **538** (2005) 33.
11) K. Yamaguchi and S. Tada: J. Electrochem. Soc. **143** (1996) 2616.
12) O. E. Tereshchenko, S. I. Chikichev and A. S. Terekhpv: Appl. Surf. Sci. **142** (1999) 75.
13) S. Kato, M. Aono, K. Sato and Y. Baba: J. Vac. Sci. Technol. A **8** (1990) 2860.
14) R. H. Fowler and L. Nordheim: Proc. R. Soc. London, Ser. A **119** (1928) 173.
15) J. S. Blakemore: J. Appl. Phys. **53** (1982) 123.
16) K. Zerrouati, F. Fabre, G. Bacquet, J. Brandet, J. Frandon, G. Lample and D. Paget: Phys. Rev. B **37** (1988) 1334.
17) M. I. D'Yakonov and V. I. Perel: Sov. Phys. JETP **33** (1971) 1053.
18) G. L. Bir, A. G. Aronov and G. E. Picus: Sov. Phys. JETP **42** (1975) 705.
19) S. Krishnamurthy: Appl. Phys. Lett. **83** (2003) 1761.
20) K. Flottmann: DESY-TESLA-FEL-97 (1997) p. 7.
21) S. Pastuszka, M. Hoppe, D. Kratzmann, D. Schwalm, A. Wolf, A. S. Jaroshevich, S. N. Kosolobov, D. A. Orlov and S. Terekhov: J. Appl. Phys. **88** (2000) 6788.
22) R. Shinohara, K. Yamaguchi, H. Hirota, Y. Suzuki, T. Manago, H. Akinaga, T. Kuroda and F. Minami: Jpn. J. Appl. Phys. **39** (2000) 7093.
23) W. Walukiewicz, J. Lagowski, L. Jastrzebski and H. C. Gatos: J. Appl. Phys. **50** (1979) 5040.
24) T. Kaneto, K. W. Kim and M. A. Littlejohn: Phys. Rev. B **47** (1993) 257.
25) S. Tiwari and S. L. Wright: Appl. Phys. Lett. **56** (1990) 563.
26) J. C. Wiesner and T. E. Everhart: J. Appl. Phys. **44** (1973) 2140.